8TH INTERNATIONAL SYMPOSIUM ON PARTICLE IMAGE VELOCIMETRY - PIV09
Melbourne, Victoria, Australia, August 25-28, 2009

Optimisation of correlation and vector averaging processes in PIV

C. R. Samarage[1], J. Carberry[2], A. Fouras[1,2] and K. Hourigan[1,2]

[1]Division of Biological Engineering, Monash University, Melbourne VIC 3800, Australia
fouras@eng.monash.edu

[2]Fluids Laboratory for Aeronautical and Industrial Research, Department of Mechanical & Aerospace Engineering, Monash University, Melbourne VIC 3800, Australia

ABSTRACT

An analysis of vector averaging and correlation averaging processes in Particle image velocimetry (PIV) has been conducted. This study has revealed the performance of correlation averaging as a function of the effective number of seed particles in an interrogation window. An optimised method of processing images for obtaining averaged measurements is introduced which utilises a combination of correlation and vector averaging processes to obtain time-averaged velocity measurements with improved accuracy. Synthetic images with varying particle densities and image noise were generated and processed using the new technique. Comparisons were made on the measurement accuracy of the optimised averaging technique with current techniques and show that at moderate seeding densities, optimised averaging is favourable.

NOMENCLATURE

σ_{PIV}	st. dev. of the PIV error (pixels)
σ_R	st. dev. of the error on the correlation plane
σ_R^1	st. dev. of correlation error for single image pair
$R_{(i,j)}$	exact correlation value at (i,j)
$R_{m,(i,j)}$	measured correlation value at (i,j)
$\varepsilon_{(i,j)}$	error of correlation value at (i,j)
u_m, u_e	measured and exact velocity components
ε_u	error of the velocity components
M	number of image pairs in an image set
N	number of image pairs in a correlation average
Q	number of vector averages for given M and N
E_n	percentage of image noise
n_p	particle seeding density over entire image
ρ_i	average number of particle images in an interrogation window contributing to the correlation function, after i averages
R	median vector rejection level
N_{ave}	number of averages in an averaging operator

1. BACKGROUND

Particle Image Velocimetry (PIV) is a non-intrusive optical technique that has been used for over two decades to obtain displacement measurements for a given flow [1]. Modern PIV techniques use high speed cameras and pulsed lasers to obtain the displacement information of seed particles over a time period. The accuracy of measurements rely on post-processing algorithms that are performed to statistically determine the displacement of the particles within an image [8].

In PIV, the velocity measurements are obtained via interrogation procedures where a set of images are divided into interrogation windows and cross-correlation is applied between successive image pairs. The resulting cross-correlation function consists of background image noise and the particle image pairs in the interrogation window [2]. With the correlation function being a probability density function (PDF), the location of the maximum peak defines the most probable location of the displacement vector and is determined via a sub-pixel interpolation technique.

Microscopic PIV (μPIV) [7], was introduced due to the increase in interest in biological flows and studying flows at a microscopic scale. A feature of μPIV [7] is the use of volume illumination, which causes a significant percentage of the particle images to be out-of-focus [4, 5]. This effect causes a distortion of the computed correlation function and reduces its signal-to-noise ratio (SNR) [8], leading to erroneous displacement measurements.

Conventional vector averaging methods work via averaging the instantaneous vector fields through the data series to yield an averaged velocity field. In cases of correlation functions with low SNR such as in μPIV, the inclusion of erroneous vectors to the averaging operator failed to yield exceptional results [3, 6]. The correlation averaging technique was developed for (μPIV) applications [3] as a means of increasing the correlation signal strength via averaging the instantaneous correlation functions to yield an averaged correlation function. Peak detection performed on the higher SNR correlation peaks resulted in more accurate displacement measurements.

This paper discusses an amalgamation of correlation averaging and vector averaging to introduce a novel algorithm. Performance analysis on this optimised averaging algorithm highlights the limitations of correlation averaging and vector averaging to derive a conclusion on the choice of technique depending on the quality of an image data set.

2. INTRODUCTION

The simplest form of obtaining time averaged measurements is vector averaging. Vector averaging averages the instantaneous vector fields through the image data series to obtain the averaged velocity field. The measurement error of vector averaging is inversely proportional to the square root of the number of averages $\sqrt{N_{ave}}$. However, if vector averaging is performed over a vector field with erroneous vectors [6], the averaged measurements obtained will be biased.

To examine the performance of vector averaging and correlation averaging techniques, a series of computer generated synthetic images were used as the raw data set. The synthetic images were of resolution 1024×1024 pixels. Noise was added to these images by generating a random number with Gaussian distribution ($\sigma = E_n = 0.5\%$ of the maximum pixel intensity). A median level vector rejection was performed post processing with a threshold of $R = 0.2$ pixels. ρ_i is defined as the number

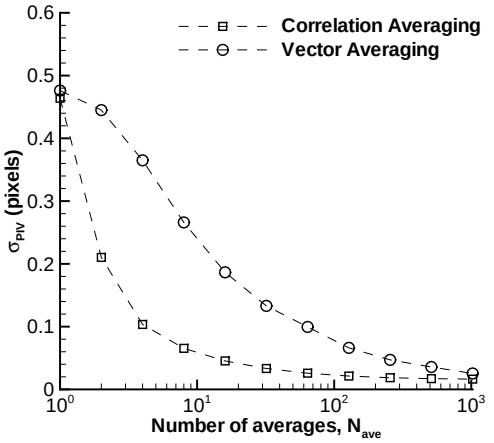

Figure 1: Comparison of the measurement accuracy versus the number of averages for current averaging techniques applied to the same series of images (low seeding density). Correlation averaging performs better at lower N_{ave} due to the exponential increase in SNR of the correlation function. The accuracy of vector averaging over M pairs approaches the correlation averaging accuracy as more vectors are included in the averaging operator.

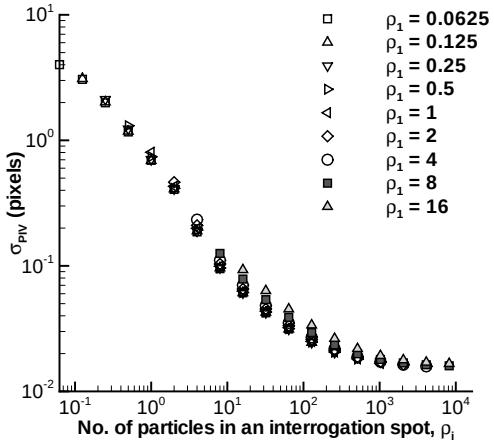

Figure 2: A plot of the standard deviation of the error in the velocity measurement (σ_{PIV}) as a function of the number of particle images in an interrogation window (ρ_i) as i is varied from $i = 1$ to M. Image series with absolute number of particles in a window (ρ_1) was varied from 0.0625 particle images per window to 16 particle images per window. We can see that the relationship is $\rho_M = \rho_1 \times N_{ave}$, since all plots overlap regardless of ρ_1.

of particle images in an interrogation window which contributes to the instantaneous correlation function after i averages. The particle seeding density per image, n_p, was varied to effectively vary the absolute number of particle images per interrogation window, ρ_1, which is for a single pair ($i = M$). ρ_1 is varied from 0.0625 particles up to 16 particles per window. For each value of ρ_1, the series consisted of $M = 1024$ image pairs and was used to vary the averaging parameters in the different techniques.

The synthetic images were analysed using the two different techniques while varying the number of averages N_{ave} to study the effect on the error in measurement accuracy σ_{PIV} (Figure 1). Correlation averaging converges more rapidly to a more accurate answer with a lower N_{ave} due to its peak strength improvement characteristics. Vector averaging converges to accuracies close to correlation averaging but at a slower rate than correlation averaging.

By definition, adding i additional images to the correlation average there is a corresponding increase in ρ_i such that $\rho_i = i\rho_1$. This effective increase in peak strength is the advantage of correlation averaging in cases of low seeding density. The vector accuracy is also improved with increasing the number of particles in an interrogation window due to its direct effect on the correlation function. This concept was evaluated through a Monte-Carlo simulation with synthetic images and is illustrated in Figure 2.

In Figure 2, σ_{PIV} is plotted as a function of ρ_i for $i = 1$ to M. Image series with different seeding densities (absolute number of particles in an interrogation window $0.0625 < \rho_1 < 16$) were correlation averaged from $N_{ave} = 1$ to $N_{ave} = M$, with increments in the number of averages included in the correlation average. It is evident that the plots of varying ρ_1 collapse for the low noise ratio case of $E_n = 0.5\%$ and it is clear the effect that increasing the number of correlation averages has on the measurement accuracy. Initially, increasing the number of averages, especially at lower and moderate ρ_i the effect of the rate of return on the decrease in error through increasing the number of averages (effective seeding density) is immense. However, as $\rho_i > 8$, this rate of decrease in the error diminishes.

We can deduce from Figure 2 that increasing the number of averages, N_{ave}, increases the number of particles in an interrogation window, ρ_i, and hence increases the measurement accuracy of correlation averaging. For varying seeding densities and for low noise conditions, the measurement accuracies obtained are similar for a given ρ_i. Therefore, we can deduce that $\rho_M = \rho_1 \times N_{ave}$.

3. OPTIMISED AVERAGING ALGORITHM

An optimised averaging algorithm is presented that combines both vector averaging and correlation averaging processes to achieve optimal results based on the signal-to-noise ratio of the instantaneous correlation function. The algorithm used to perform this optimised averaging technique on an image set is shown in Figure 3.

This algorithm performs a correlation average over only a sub-set N, of the instantaneous correlation functions. Peak detection is then performed on the averaged correlation functions and the resulting vector fields are vector averaged. The sub-set number of pairs in a correlation average, N, is varied from $N = 1$, which signifies complete vector averaging where the number of vector averages $Q = M$, to $N = M$ for complete correlation averaging where $Q = 1$. Any other value for N in between 1 and M defines an optimised averaging which uses a ratio of correlation averaging to vector averaging. The inclusion of complete vector and correlation averaging for values of N enable us to perform comparisons on how varying optimized averages perform again vector and correlation averaging.

From Figure 2, we deduced that $\sigma_{PIV} \propto \frac{1}{\sqrt{\rho_i}}$ from the performance analysis on correlation averaging. Varying the number of pairs in a correlation average, N, in optimised averaging has a similar effect on the effective seeding density

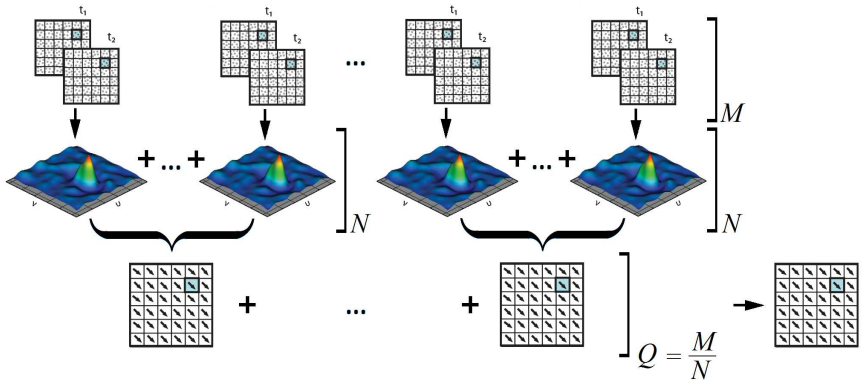

Figure 3: Graphical representation of the optimised averaging algorithm. The technique is applied to an image series of M image pairs whereby a subset N is correlation averaged. The resulting M/N pairs (Q) are then vector averaged to obtain the averaged velocity measurement.

and hence the correlation function quality. A study was performed on synthetic images for cases of $1 < N < M$ and $0.0625 < \rho_i < 16384$.

As $\rho_1 < 0.5$, correlation averaging proves that it can yields the optimal results as shown in Figure $4(a)$. Increasing the number of pairs in a correlation average, and thus reducing Q, minimises the error in the PIV measurement. This is because of the effect of the peak strengthening characteristics of correlation averaging, on correlation peaks with low signal strength inherent at low seeding densities. Figure $4(a)$ illustrates the case in which σ_{PIV} is not a function of N as $N >> 16$. As $\rho_1 > 8$, vector averaging produces a vector measurement with the least error as shown in Figure $4(c)$. Since $\rho_i > 8$, the stronger correlation function peaks yield more accurate vectors and peak detection is dominant over peak strengthening. For cases of $0.5 < \rho_1 < 8$, correlation averaging to a certain point followed by vector averaging works better compared to correlation averaging alone.

Figure $4c$ illustrates that as the number of images pairs in a correlation average N increase above a certain threshold, the signal strength is high enough for vector averaging to be performed and has a diminished effect on σ_{PIV}. However, the optimised averaging method performs better than correlation averaging for the intermediate seeding density cases.

4. STATISTICAL ANALYSIS

An extensive error analysis was performed to better define the error measurement variables. The equation for a three-point estimator at the sub-pixel level used to determine the peak location in the correlation function is based on a parabolic peak fit estimator [6] as shown in Eq: 1.

$$u_e = \frac{R_{(i-1,j)} - R_{(i+1,j)}}{2R_{(i-1,j)} - 4R_{(i,j)} + 2R_{(i+1,j)}}, \tag{1}$$

where $R_{(i,j)}$ is the peak correlation value in the correlation plane.

The exact correlation values, R, are based on an ideal correlation function obtained through auto-correlation of an *ideal* synthetic image with image noise $E_n = 0\%$, and high seeding density, where $\rho_1 >> 8$ to ensure ideal correlation SNR. The correlation function of the measurements has an error $\varepsilon_{(i,j)}$ associated where the measured correlation values is defined by $R_{m,(i,j)}$.

$$R_{m,(i,j)} = R_{(i,j)} + \varepsilon_{(i,j)}, \tag{2}$$

An error term in the peak signifies an error term in the velocity measurement. This velocity measurement error, ε_u, is the difference between the measured velocity component and the exact velocity component from the exact peak (Eq: 3).

$$\varepsilon_u = u_m - u_e, \tag{3}$$

σ_{PIV} describes the error in measured velocity components due to the variation of the measured correlation function and is defined as the standard deviation of the error in the velocity component, ε_u. The measured value for the velocity component, u_m, is obtained by subtituting Eq: 2 into Eq: 1. Upon substituting the resulting equation for u_m into Eq: 3, the result is expanded and resolved through neglecting terms of least significance.
By use of a statistics manipulation for two linearly dependent variables, the expanded equation of Eq: 3 can be converted to an equation such that we can relate the standard deviation of the velocity component, σ_{PIV}, to the standard deviation of the error in the correlation function, σ_R.

$$\sigma_{PIV} = K \times \sigma_R, \tag{4}$$

where the proportionality constant for the correlation peak, K, is defined as shown in Eq: 5.

$$K = \frac{\sqrt{2(R^2_{(i-1,j)} + R^2_{(i,j)} + R^2_{(i+1,j)})}}{D}, \tag{5}$$

$$\text{and} \quad D = 4[(R_{(i-1,j)} + R_{(i+1,j)})^2 + 4R_{(i,j)}(-R_{(i-1,j)} + 4R_{(i,j)} - R_{(i+1,j)}),$$

Let the standard deviation of the correlation value error for a single pair of images ($M = 1$), be defined as σ^1_R. Given a set of image pairs (M), the post-processing method may involve N correlation averages. Based on M and N, the number of vector averages involved in the processing stage is $Q = \frac{M}{N}$.
As $M > 1$, the error in the correlation peak values, σ_R, decreases since the correlation peak is strengthened as more pairs are correlation averaged in the technique.

$$\sigma_R = \frac{\sigma^1_R}{\sqrt{N}}, \tag{6}$$

From Eq: 4:

$$\sigma^1_{PIV} = K\frac{\sigma^1_R}{\sqrt{N}}, \tag{7}$$

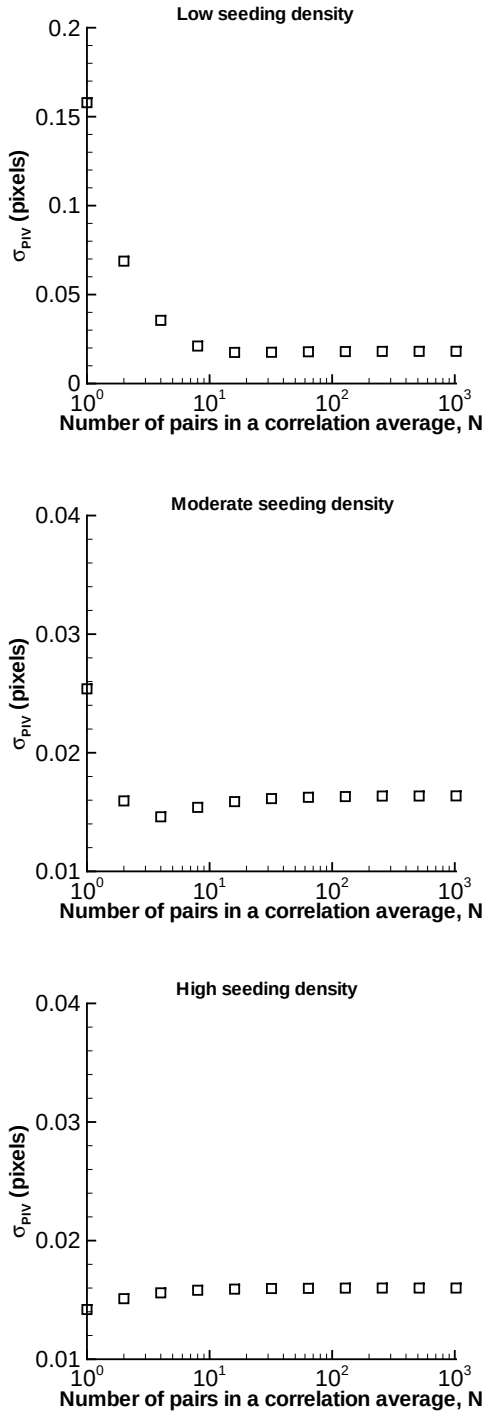

Figure 4: Plots of the standard deviation of the velocity measurement error (σ_{PIV}) as a function of the absolute seeding density of an image series (ρ_1). Image noise constant at $E_n = 0.5\%$. Depending on ρ_1, the different averaging techniques perform differently. In cases of a $\rho_i < 1$ (TOP), correlation averaging performs much better than vector averaging. In cases of high seeding density, $\rho_1 > 8$ (BOTTOM), complete vector averaging performs better than complete correlation averaging. In the case of images with moderate seeding densities, $1 < \rho_1 < 8$ (MIDDLE) the optimized averaging with both correlation/vector averaging over 1024 pairs performs over complete correlation averaging by 13.67%.

Likewise, the increase in vector averages would have a similar effect on the velocity measurement error σ_{PIV}. Simplifying Eq: 7, further using $Q = \frac{M}{N}$, we obtain Eq: 8.

$$\sigma_{PIV} = K\frac{\sigma_R^1}{\sqrt{Q}\sqrt{N}} = K\frac{\sigma_R^1}{\sqrt{M}}, \tag{8}$$

Eq: 8 shows that σ_{PIV} is no longer a function of N, as evident in figure 4 when N is increased. As N is increased, the error in the peak is minimised and the measurement accuracy is not affected by the discrepancies in peak detection. Therefore, the standard deviation of the vector measurement is no longer fully modeled by sub-pixel interpolation. The velocity measurement accuracy is dependent on the right location and strength of the correlation peak.

5. CONCLUSION

An optimised averaging algorithm was proposed that uses both vector averaging and correlation averaging techniques to better utilise the effective ρ_i. A study of the optimised averaging technique was conducted by using synthetic images that simulate PIV experimental images under low noise levels. Optimised averaging is based on increasing the number of correlation averages until the optimal correlation function signal strength is reached before performing a vector average. The effective ρ_i determines the technique required for optimal results. The results showed that vector averaging performed better in cases with high seeding densities, while correlation averaging performed better in cases of low seeding densities. However, in cases where $0.5 < \rho_1 < 8$ the optimised averaging technique showed improved accuracy with accuracies up to 15% better than correlation averaging.

This optimised averaging technique shows great promise in better utilising vector averaging and correlation averaging algorithms to obtain the most accurate velocity measurements for cases where time averaged measurements are required.

ACKNOWLEDGMENTS

Support from an Australian Research Council Discovery Grant (ARC DP0877327) is gratefully acknowledged.

REFERENCES

[1] Adrian, R. J., (2004), *12th Intl. Symposium on App. of Laser Techniques to Fluids Mech., Lisbon, Portugal*

[2] Keane, R. D., Adrian, R. J., (1992), *App. Sci. Research*, **49**, pp. 191-215

[3] Meinhart, C. D., Wereley, S. T., Santiago, J. G., (2000), *Journal of Fluids Eng.*, **122**, pp. 285-289

[4] Olsen, M. G., and Adrian, R. J., (2000), *Exp. Fluids*, **27**, pp. S166-S174

[5] Olsen, M. G., and Bourdon, C. J., (2003), *Journal of Fluids Eng.*, **125**, pp. 895-901

[6] Raffel, M., Willert, C. E., Wereley, S. T., and Kompenhans, J., (2007), *Springer, Berlin*, (ISBN: 978-3-540-72307-3)

[7] Santiago, J. G., Wereley, S. T., Meinhart, C. D., Beebe, D. J., and Adrian, R. J., (1998), *Exp. Fluids*, **25**, No.4, pp. 316-319

[8] Westerweel, J., (1998), *Meas. Sci. Technol.*, **8**, pp. 1379-1392